Leaf-inspired interwoven carbon nanosheet/nanotube homostructure for supercapacitors with high energy and power densities

Siliang Liu,[a] Jingsan Xu,[b] Jixin Zhu,[c] Yuanqin Chang,[d] Haige Wang,[a] Zhichong Liu,[a] Yang Xu,[a] Chao Zhang*[a] and Tianxi Liu*[a]

[a] State Key Laboratory for Modification of Chemical Fibers and Polymer Materials, College of Materials Science and Engineering, Donghua University, Shanghai 201620, P. R. China

[b] School of Chemistry, Physics and Mechanical Engineering, Queensland University of Technology, Brisbane, QLD 4001, Australia

[c] Key Laboratory of Flexible Electronics (KLOFE) & Institute of Advanced Materials (IAM), Jiangsu National Synergetic Innovation Center for Advanced Materials (SICAM), Nanjing Tech University, 30 South Puzu Road, Nanjing 211816, China

[d] CAT Catalytic Center, RWTH Aachen University, Worringerweg 2, D-52074 Aachen, Germany

* E-mail: czhang@dhu.edu.cn (C. Zhang)

* E-mail: txliu@fudan.edu.cn or txliu@dhu.edu.cn (T. X. Liu)

Electronic Supplementary Information

Figure captions:

Fig. S1 SEM images of (a, b) CNSs and (c, d) CNTs at low and high magnifications, respectively.

Fig. S2 SEM images of (a, b) CNT-CNS-1, (c, d) CNT-CNS-2 and (e, f) CNT-CNS-3 at low and high magnifications, respectively.

Fig. S3 SEM images of leaf-inspired interwoven CNT-CNS-2 at different magnifications.

Fig. S4 HETEM images of (a-c) CNSs, (d-f) CNT-CNS-2 at different magnifications.

Fig. S5 Elemental compositions of CNTs, CNT-CNS sandwiches and CNSs.

Fig. S6 (a) XPS survey spectra of CNT-CNS-1 and CNT-CNS-3. C1s XPS spectra of (b) CNT-CNS-1 and (c) CNT-CNS-3.

Fig. S7 (a) Nitrogen adsorption-desorption isotherms and (b) pore size distributions of CNT-CNS-1 and CNT-CNS-3, respectively.

Fig. S8 (a) Comparison of CV curves of CNT-CNS-4 and CNT-CNS-5 at a scan rate of 10 mV s^{-1}. (b) Specific capacitances of CNT-CNS-4 and CNT-CNS-5 at various discharge current densities.

Fig. S9 (a) Comparison of CV curves of neat graphite paper at a scan rate of 10 mV s^{-1}. (b) Specific capacitances of neat graphite paper at various discharge current densities.

Fig. S10 Ragone plots for assembled symmetric supercapacitors with CNT-CNS sandwiches.

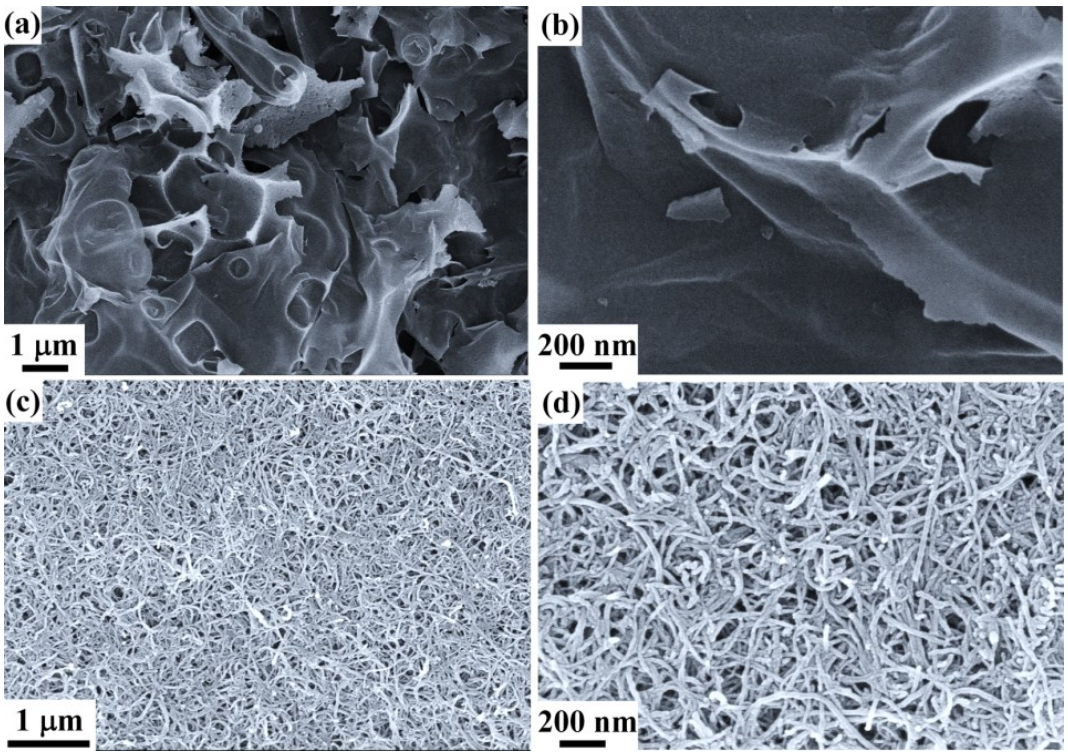

Fig. S1 SEM images of (a, b) CNSs and (c, d) CNTs at low and high magnifications, respectively.

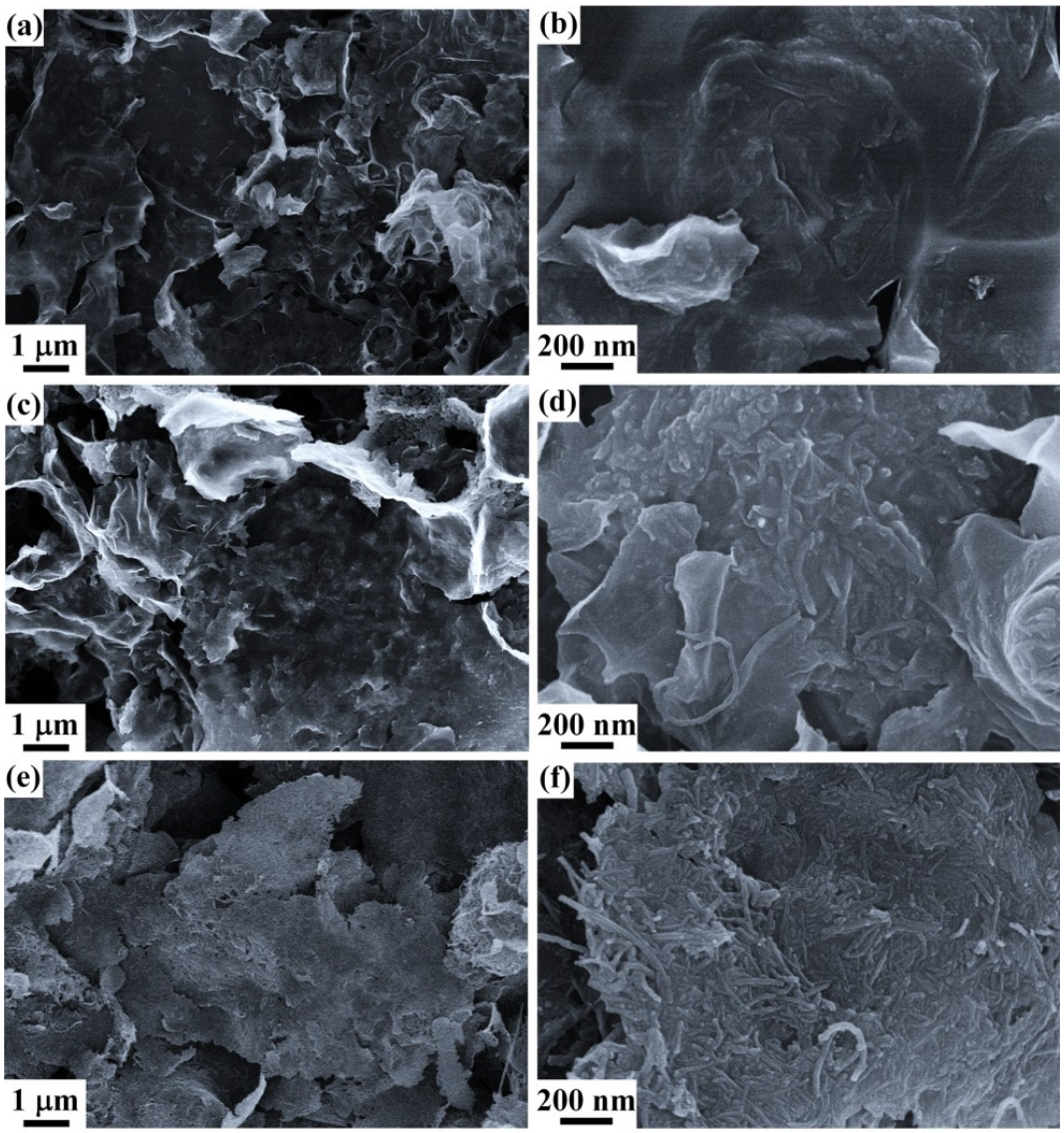

Fig. S2 SEM images of (a, b) CNT-CNS-1, (c, d) CNT-CNS-2 and (e, f) CNT-CNS-3 at low and high magnifications, respectively.

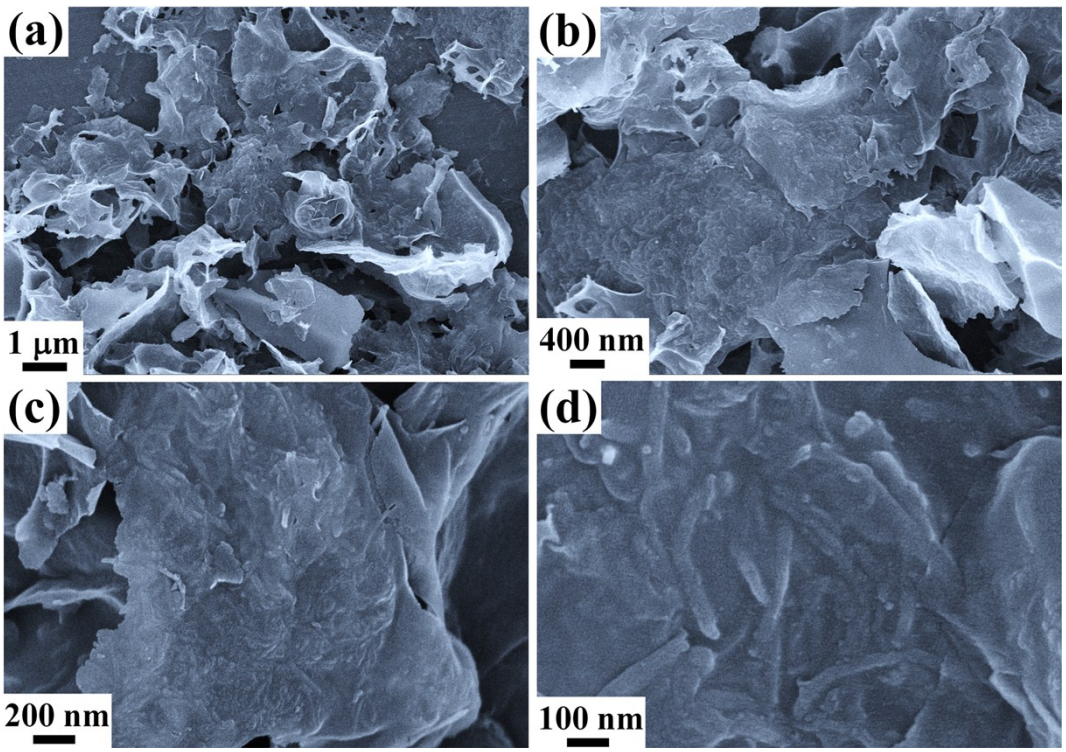

Fig. S3 SEM images of leaf-inspired interwoven CNT-CNS-2 at different magnifications.

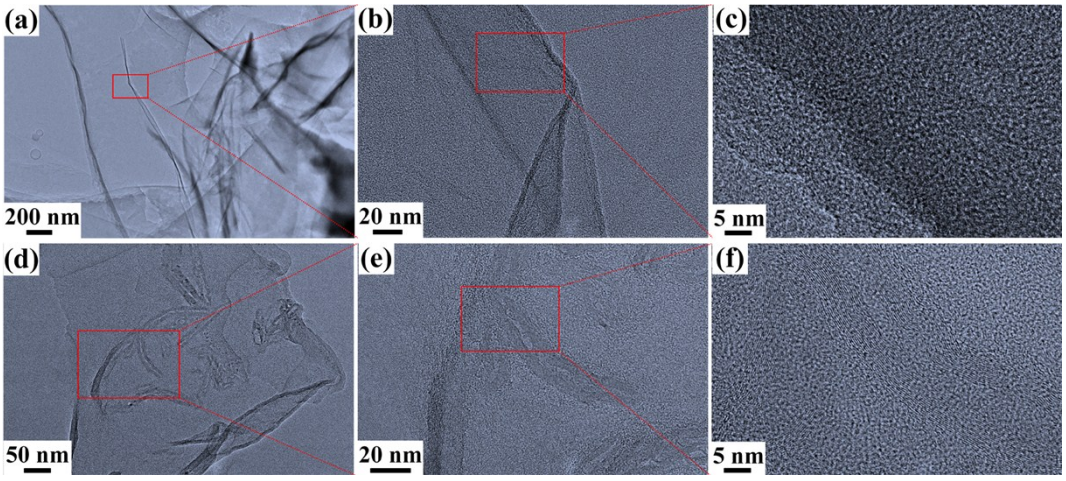

Fig. S4 HETEM images of (a-c) CNSs, (d-f) CNT-CNS-2 at different magnifications.

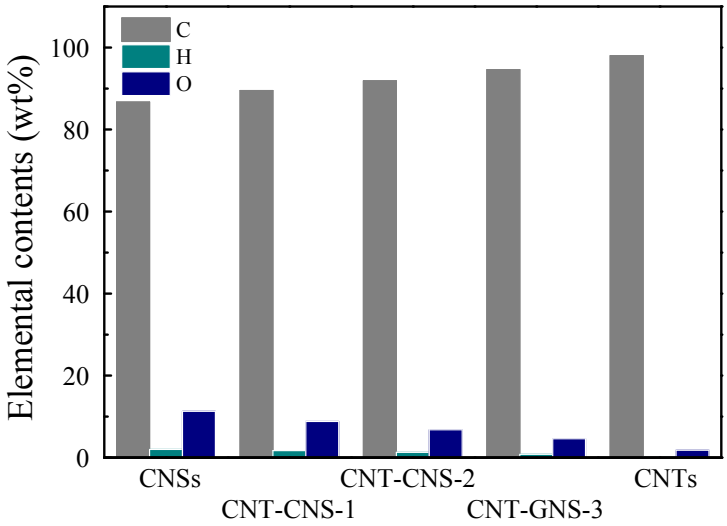

Fig. S5 Elemental compositions of CNTs, CNT-CNS sandwiches and CNSs.

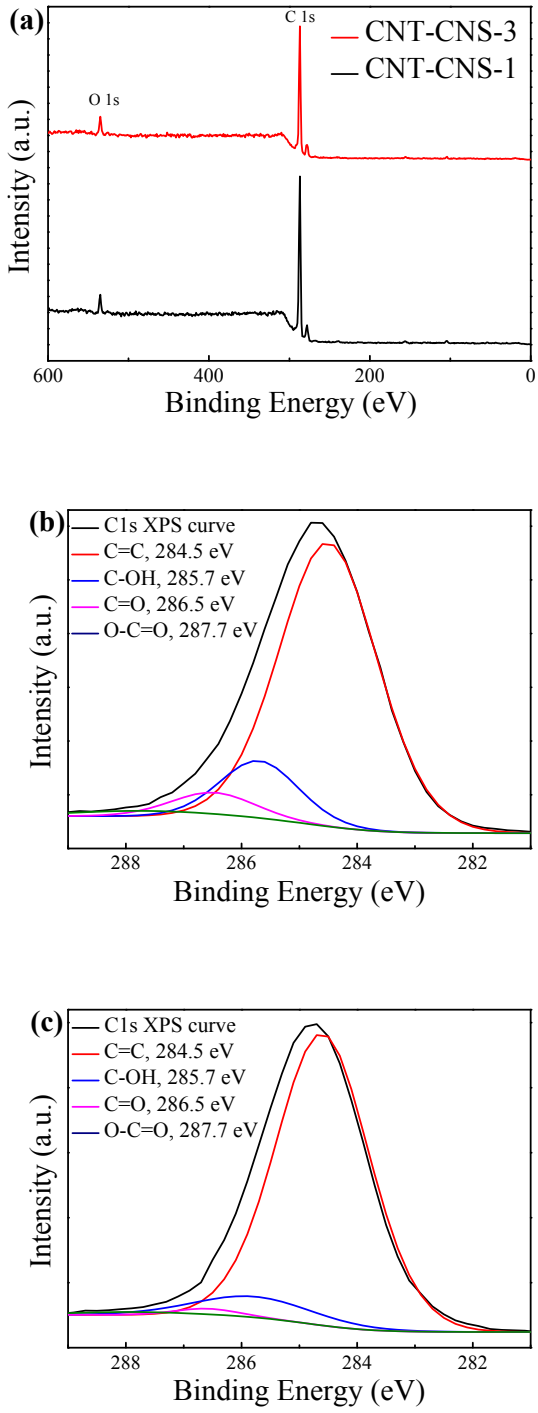

Fig. S6 (a) XPS survey spectra of CNT-CNS-1 and CNT-CNS-3. C1s XPS spectra of (b) CNT-CNS-1 and (c) CNT-CNS-3.

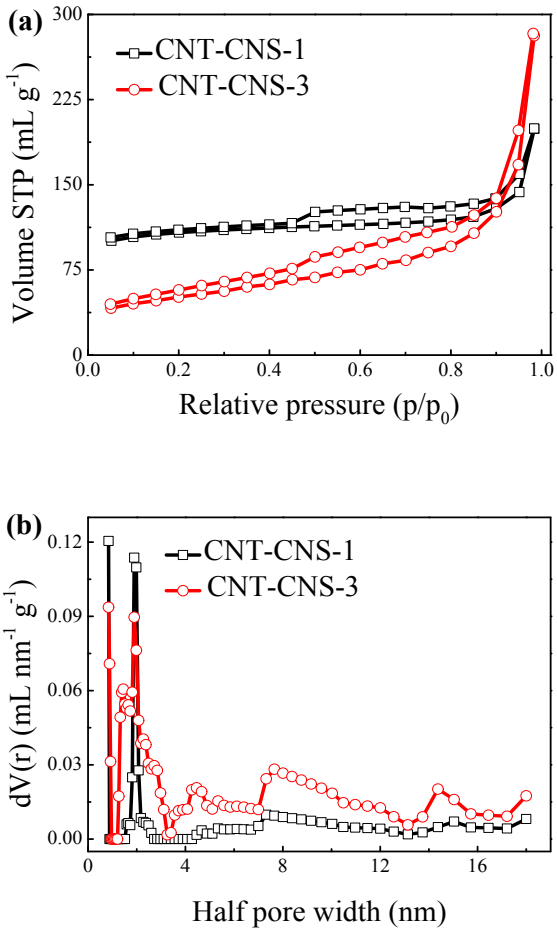

Fig. S7 (a) Nitrogen adsorption-desorption isotherms and (b) pore size distributions of CNT-CNS-1 and CNT-CNS-3, respectively.

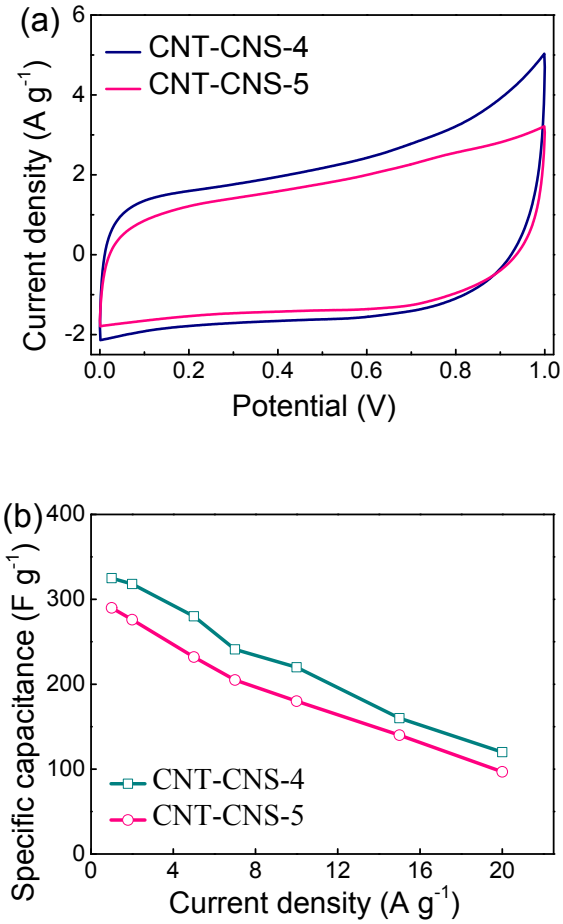

Fig. S8 (a) Comparison of CV curves of CNT-CNS-4 and CNT-CNS-5 at a scan rate of 10 mV s^{-1}.

(b) Specific capacitances of CNT-CNS-4 and CNT-CNS-5 at various discharge current densities.

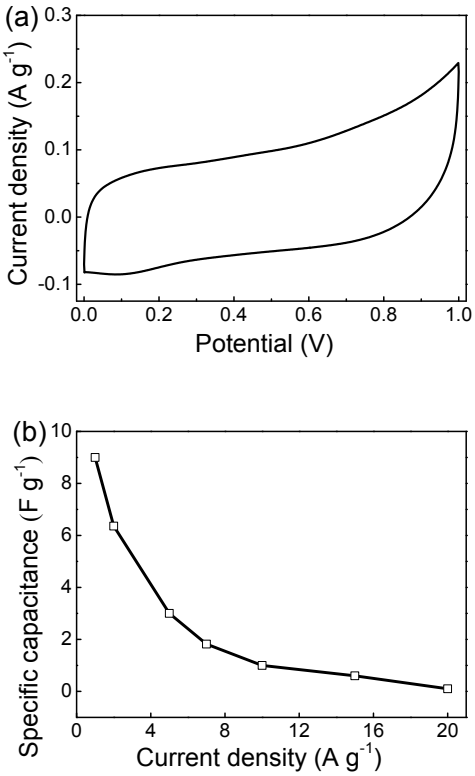

Fig. S9 (a) Comparison of CV curves of neat graphite paper at a scan rate of 10 mV s^{-1}. (b) Specific capacitances of neat graphite paper at various discharge current densities.

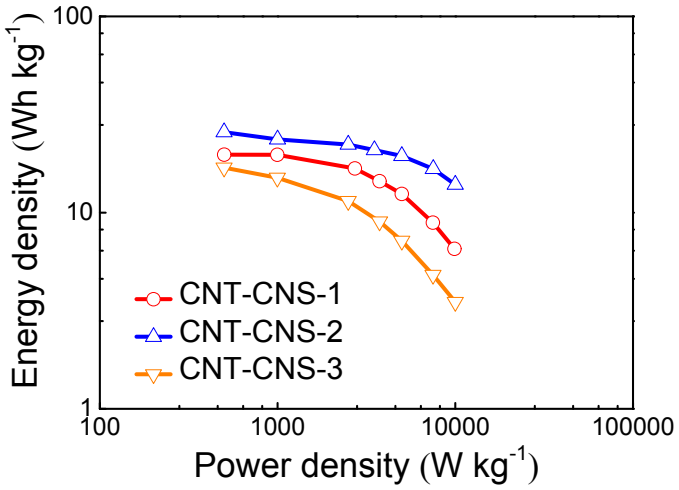

Fig. S10 Ragone plots for assembled symmetric supercapacitors with CNT-CNS sandwiches.

Table S1. The electrical conductivity parameters of CNSs, CNT-CNS sandwiches and CNTs.

Sample	Resistivity [Ω cm]	Conductivity [S m^{-1}]
CNSs	4.92	21
CNT-CNS-1	3.33	30
CNT-CNS-2	2.28	44
CNT-CNS-3	1.56	64
CNTs	0.07	1428